

## ***Supplementary Material***

### **Supplementary Figures and Tables**

**Supplementary Table 1A.** Strains used in this study.

Strain	Genotype	Source or Reference
MG1655	K-12 F <sup>-</sup> λ <sup>-</sup> rph-1	(Blattner et al., 1997)
HDB51	WAM113 secB <sup>+</sup> zic-4901::Tn10	(Lee and Bernstein, 2001)
MY1410	MG1655 <i>fjh</i> ::Cm <sup>r</sup> , pKDFB	(Zhao et al., 2021)
MY1901	MG1655 <i>fjh</i> :: Cm <sup>r</sup> , C3453283T	This study
MY1901F	MY1901, pTrc99K-Ffh	This study
MY1901FS	MY1901F, T3453283C	This study
MY1901Δcat	MY1901, Δcat	This study
MG1655ΔlacZ	MG1655, ΔlacZ	(Zhao et al., 2021)
MY1901ΔlacZΔcat	MY1901, ΔlacZΔcat	This study

**Supplementary Table 1B.** Plasmids used in this study.

Plasmid	Relevant genotype	Source or Reference
pTrc99K-Ffh	pTrc99K, P <sub>trc</sub> - <i>ffh</i> , Km <sup>r</sup>	(Zhao et al., 2021)
pKUT15-fusA-lacZα	OriSC101 lacIq P <sub>lac</sub> - <i>fusA-lacZα</i> , P <sub>ter</sub> - <i>lacZω</i> , Gm <sup>r</sup>	(Dai et al., 2018)
pKUT15-lacZα	pKUT15, P <sub>lac</sub> - <i>lacZα</i> , P <sub>ter</sub> - <i>lacZω</i>	(Zhao et al., 2021)
pKUT15-msbA-lacZα	pKUT15, P <sub>lac</sub> - <i>msbA-lacZα</i> , P <sub>ter</sub> - <i>lacZω</i>	(Zhao et al., 2021)
pLacZ	pTrc99K, P <sub>trc</sub> - <i>lacZ</i>	This study
pLacZ <sub>835UAA</sub>	pLacZ, UAA mutant	(O'Connor et al., 1992)
pLacZ <sub>12-6UAG</sub>	pLacZ, UAG mutant	(O'Connor et al., 1992)
pLacZ <sub>34-11UGA</sub>	pLacZ, UGA mutant	(O'Connor et al., 1992)
pLacZ <sub>lac10(-)</sub>	pLacZ, -1 frameshift	(O'Connor et al., 1992)
placZ <sub>lac7(+)</sub>	pLacZ, +1 frameshift	(O'Connor et al., 1992)
pRed_Cas9_ApoxB300	OrirepA101, exo, bet, gam, arabinose operon, Cas9, gRNA, Ap <sup>r</sup>	(Zhao et al., 2016)
pGFP	pTrc99K, P <sub>trc</sub> -gfp <sub>AUG</sub>	This study
pGFP <sub>GUG</sub>	pTrc99K, P <sub>trc</sub> -gfp <sub>GUG</sub>	This study
pGFP <sub>UUG</sub>	pTrc99K, P <sub>trc</sub> -gfp <sub>UUG</sub>	This study
pGFP <sub>AUA</sub>	pTrc99K, P <sub>trc</sub> -gfp <sub>AUA</sub>	This study
pGFP <sub>AUU</sub>	pTrc99K, P <sub>trc</sub> -gfp <sub>AUU</sub>	This study
pGFP <sub>AUGmetYCAU</sub>	pGFP, expressing tRNA <sup>fMet</sup> with CAU anticodon	This study
pGFP <sub>UAGmetYCAU</sub>	pGFP <sub>AUGmetYCAU</sub> , AUG initiation codon mutated to UAG and anticodon of metY was changed from CAU to CUA	This study
pGFP <sub>CACmetYGUG</sub>	pGFP <sub>AUGmetYCAU</sub> , AUG initiation codon mutated to CAC and anticodon of metY was changed from CAU to GUG	This study
pGFP <sub>UACmetYGUA</sub>	pGFP <sub>AUGmetYCAU</sub> , AUG initiation codon mutated to UAC and anticodon of metY was changed from CAU to	This study

	GUA	
Cas9-S10 SD	pRed Cas9 ΔpoxB300, homologous arms of SD of S10	This study
Cas9-lacZ	pRed Cas9 ΔpoxB300, homologous arms of lacZ	(Zhao et al., 2021)
Cas9-cat	pRed Cas9 ΔpoxB300, homologous arms of cat	(Zhao et al., 2021)
p15A-birA	Orip15A, lacIq P <sub>tac</sub> -birA, Gm <sup>r</sup>	This study
pJH29-EspP-PSBT	pJH29, P <sub>tac</sub> -espP, PSBT-FLAG, Cm <sup>r</sup>	(Zhang and Shan, 2012)
pJH29-EspP-Avi	pJH29, P <sub>tac</sub> -espP, Avi-FLAG, Cm <sup>r</sup>	This study
pJH29-FtsQ-Avi	pJH29, P <sub>tac</sub> -ftsQ, Avi-FLAG, Cm <sup>r</sup>	This study
pJH29-LacZ-Avi	pJH29, P <sub>tac</sub> -lacZ, Avi-FLAG, Cm <sup>r</sup>	This study
pJH30-EspP-PSBT	pJH29, lac operon replaced with araC operon, Ap <sup>r</sup>	(Zhao et al., 2021)
pJH30-SD-GFP	pJH30, P <sub>araBAD</sub> -GFP, wild-type SD, Ap <sup>r</sup>	This study
pJH30-SD*-GFP	pJH30, P <sub>araBAD</sub> -GFP, mutant SD, Ap <sup>r</sup>	This study
pJH31-SD-GFP	pJH30, P <sub>araBAD</sub> replaced with P <sub>S10</sub> , wild-type SD Ap <sup>r</sup>	This study
pJH31-SD*-GFP	pJH31, P <sub>S10</sub> -GFP, mutant SD, Ap <sup>r</sup>	This study

**Supplementary Table 1C. Primers used in this study.**

Primer	Sequence (5'→3')	Use
pTrc99K-F	GATCCTCTAGAGTCGACCT	Cloning of the vector bone of plasmid pTrc99K
pTrc99K-R	GAGCTCGAATTCCATGGTCT	
GFP-F	ACAGACCAGATGGAATTCTGAGCTCATGAGTA AAGGGAGAAGAACTTTTC	Cloning of gfp segment
GFP-R	TGCAGGTCGACTCTAGAGGATCCTATTG TATAGTTCATCCATG	
GFP <sub>GUG</sub> -F	ACAGACCAGATGGAATTCTGAGCTCGTGAGT AAAGGGAGAAGAACTTTTC	Cloning of gfp <sub>GUG</sub> with segment
GFP <sub>UUG</sub> -F	ACAGACCAGATGGAATTCTGAGCTCTTGAGT AAAGGGAGAAGAACTTTTC	Cloning of gfp <sub>UUG</sub> with segment
GFP <sub>AUA</sub> -F	ACAGACCAGATGGAATTCTGAGCTCATAAGT AAAGGGAGAAGAACTTTTC	Cloning of gfp <sub>AUA</sub> with segment
GFP <sub>AUU</sub> -F	ACAGACCAGATGGAATTCTGAGCTCATTAGT AAAGGGAGAAGAACTTTTC	Cloning of gfp <sub>AUU</sub> with segment
MetY-V-R	GTGAAAACCTCTGACACATG	Cloning of the vector bone of plasmid pGFP with primer pTrc99K-F
MetY <sub>CAU</sub> -F	CTGCATGTGTCAGAGGTTTCACTGGAT CACTATAATGCCTGC	Construction of plamid pGFP <sub>AUG</sub> metY <sub>CAU</sub>
MetY <sub>CAU</sub> -R	CTATCATGCCATACCGCGAAAGGAGCC CAGTTATTCTGTAGTC	
MetY-V-F	CCTTCGCGGTATGGCATG	
MetY <sub>CUA</sub> -F	GTCGGGCTCTAACCCGAAGATCGT	Construction of plamid pGFP <sub>UAG</sub> metY <sub>CUA</sub>
MetY <sub>CUA</sub> -R	ACGATCTCGGGTTAGAGCCCCGACG	
GFP <sub>UAG</sub> -F	ACAGACCAGATGGAATTCTGAGCTCTAGAGTAA AGGAGAAGAACTTTTC	
MetY <sub>GUG</sub> -F	GTCGGGCTGTAAACCCGAAGATCGT	Construction of plamid pGFP <sub>CAC</sub> metY <sub>GUG</sub>
MetY <sub>GUG</sub> -R	ACGATCTCGGGTTAGAGCCCCGACG	
GFP <sub>CAC</sub> -F	ACAGACCAGATGGAATTCTGAGCTCCACAGTAA AGGAGAAGAACTTTTC	
MetY <sub>GUA</sub> -F	GTCGGGCTGTAAACCCGAAGATCGT	Construction of plamid pGFP <sub>UAC</sub> metY <sub>GUA</sub>
MetY <sub>GUA</sub> -R	ACGATCTCGGGTTAGAGCCCCGACG	
GFP <sub>UAC</sub> -F	ACAGACCAGATGGAATTCTGAGCTCTACAGTAA AGGAGAAGAACTTTTC	
V1-cas9-F	TGAATGGAAGCTGGATTCTC	Cloning of the vector bone 1 of plasmid Cas9-S10 SD
V1-S10-R	TATCCGCCTGAAAGCGTTGGCTAAGATCTG ACTCCATAAC	

V2-S10-F	CAAACGCTTCAGGCGGATAGTTTAGAGCT AGAAATAGCAAG	Cloning of the vector bone 2 of plasmid Cas9-S10 SD
V2-cas9-R	ACAGGCCCATGGATTCTCG	
S10-UP-F	CGAAGAATCCATGGGCCTGTTAACCCAGG CTGATCTGC	Cloning of the upstream of the mutated site
S10-UP-R	CTGGTCTCATGCAGAACCAAAGAACGTAT CC	
S10-DN-F	TGGTTCTGCATGAGACCAGAGCTCCAATTAT	Cloning of the downstream of the mutated site
S10-DN-R	AGAATCCAAGCTTCCATTCAAAGAGAAAGC CGGTTAACAGAG	
p15-V-F	CCCAGGCATCAAATAAAACG	Cloning of the vector bone of plasmid p15A-birA
p15-V-R	GATCCGAATTCTGCAGTTG	
birA-F	TAACAACGTGAGGAATTGGATCATGAAGG ATAACACCGTGCC	Cloning of the <i>birA</i> segment
birA-R	TTTCGTTTATTGATGCCTGGTTATTTTC TGCCTACCGCAG	
29-V-F	TTCCGGCTTGAAACGACATCTCGAGGCCA GAAGATCGAGTGGCACGAGGGTCTGGTGA CTACAAAGACGATGACGAC	Cloning of the vector bone of plasmid pJH29-EspP-Avi from pJH29-EspP-PSBT
29-V-R	ATTAGTCCGCCAGTTCCAC	
espP-F	TATGTGGAACTGGCGGACTAATATGAATAAA ATATACTCTC	Cloning of the <i>espP</i> segment
espP-R	CGAAGATGTCGTTCAAGCCGGAACCGATATA GTCAGCAGTATTATT	
FtsQ-Avi-V-F	CTTCGAGGCCAGAACGATCGAGTGGCACGA GGGTTCTGGTGAACAAAGACGATGACGA C	Cloning of the vector bone of plasmid pJH29-FtsQ-Avi from pJH29-EspP-Avi with primer 29-V-R
FtsQ-Avi-F	TATGTGGAACTGGCGGActaatATGTCGCAGGC TGCTCTG	Cloning of the <i>ftsQ-Avi</i> tag segment
FtsQ-Avi-R	ACTCGATCTCTGGGCCTCGAACGATGTCGTT CAAGCCTCTAGATTGTTCTGCCTGTGCC T	
LacZ-Avi-V-F	TTCCGGCTTGAAACGACATCT	Cloning of the vector bone of plasmid pJH29-LacZ-Avi from pJH29-EspP-Avi with primer 29-V-R
LacZ-Avi-F	ATGTGGAACTGGCGGACTAATATGACCATGA TTACGGATTAC	Cloning of the <i>lacZ-Avi</i> tag segment
LacZ-Avi-R	AAGATGTCGTTCAAGCCGGAACCTTTTGAC ACCAGACCAACTG	
pJH30-F	ATCAGTAAGTTGGCAGCATC	Cloning of the vector bone of plasmid pJH30
pJH30-R	ATGGAGAAACAGTAGAGAGAGTTG	
S10 leader-F	CAACTCTACTGTTCTCCATGGCTACCTA ACAATGCTCC	Cloning of the S10 leader containing SD from MG1655 genome (wild-type SD) or MY1901 genome (mutant SD)
S10 leader-R	AAAGTTCTCTCCTTACTCATCGGATACGG ATTCTTGGTCTG	
GFP-F	ATGAGTAAAGGAGAAGAACTTTC	Cloning of the <i>gfp</i> segment
GFP-R	TGATGCTGCCAACTTACTGATCTATTGTATA GTTCATCCATG	
pJH31-R	CGCGGAACCCCTATTGTT	Cloning of the vector bone of plasmid pJH31 with primer pJH30-F
P <sub>S10</sub> -F	AATAAACAAATAGGGTCCGGAGCGTG TCAAAAATGCACTG	Cloning of the P <sub>S10</sub> promoter and S10 leader containing SD from MG1655 genome or MY1901 genome

**Supplementary Table 2. Summary of single nucleotide variants (SNVs), and insertions and deletions (INDELS).** The strain MY1901 shared common mutations with the original strain MG1655 in the laboratory, except the mutation located in the Shine-Dalgarno (SD) sequence of ribosome S10 operon. The evolved strain MY1901 by sub-culturing showed new mutations.

Strain	Mutation site	Type	Chrom Start	chrom END	Ref	Obs	Relative to original strain
MY1901	<i>fhuA</i>	SNV	168123	168123	A	C	
	<i>ybhJ</i>	SNV	803662	803662	C	A	
	<i>mntP</i>	SNV	1905761	1905761	G	A	
	<i>yjbI</i>	SNV	4251856	4251856	T	C	
	<i>gatC</i>	INDEL	2173363	2173364	CC	-	
	<i>glpR</i>	INDEL	3560455	3560455	-	G	
	<i>Promoter yagEp3</i>	SNV	282234	282234	G	T	
	<i>A repetitive extragenic palindromic (REP) element downstream of yjcO</i>	INDEL	4296381	4296381	-	GC	
	<i>Shine-Dalgarno (SD) sequence of ribosome S10 operon</i>	SNV	3453283	3453283	C	T	unique
MY1901 (evolved)	<i>rpsJ</i>	SNV	3453146	3453146	A	C	
	<i>DnaA</i>	SNV	3882819	3882819	G	T	
	<i>rpoB</i>	SNV	4182952	4182952	G	A	
	<i>rpoC</i>	SNV	4186367	4186367	C	A	

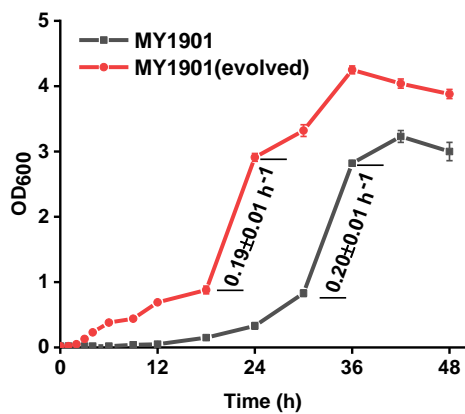
Ref = reference allele; Obs = observed allele.

**Supplementary Table 3. Growth rate and the time cost of initiation steps ( $T_{init}$ ) of cells under different nutrient conditions.** Growth rates were calculated from the corresponding growth curves that were shown in Supplementary Figure S4. All values are expressed as the mean  $\pm$  standard deviation of the mean of samples. The initiation time ( $T_{init}$ ) was calculated as described in the Materials and Methods section.

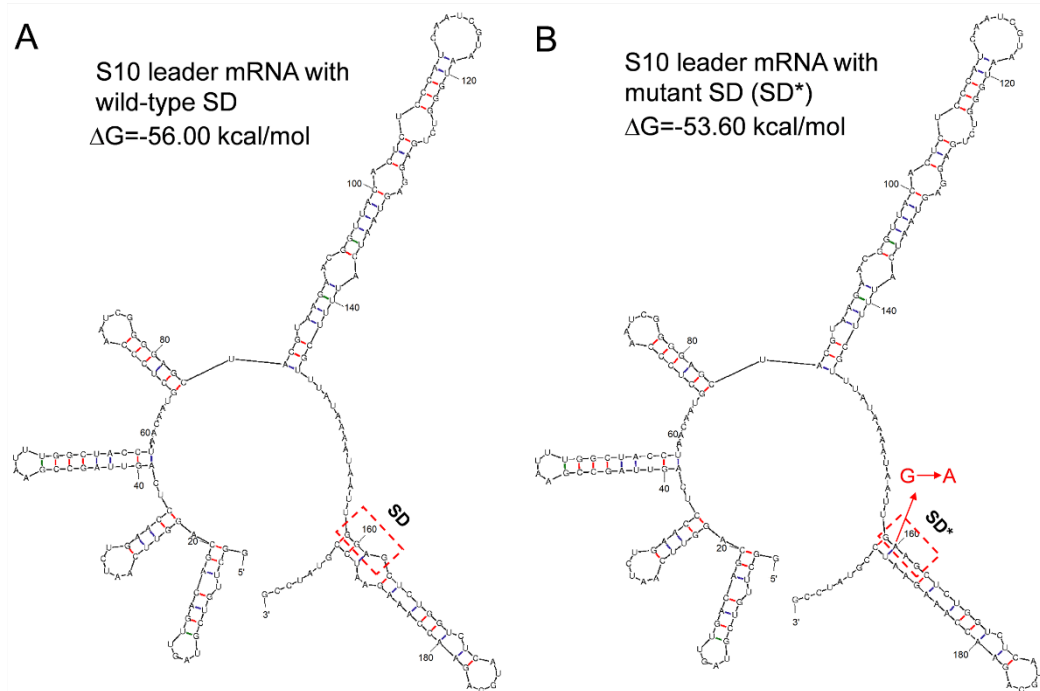
Strain	Nutrient condition	Growth rate ( $\text{h}^{-1}$ )	$T_{int}$
MG1655 $\Delta lacZ$	Glucose + cAA	$1.10 \pm 0.04$	$10.0 \pm 0.2$ (FusA)
	0.2% glucose + 0.2% casamino acids		$9.6 \pm 0.2$ (MsbA)
MG1655 $\Delta lacZ$	Glycerol + NH <sub>4</sub> Cl	$0.55 \pm 0.03$	$9.6 \pm 0.2$ (FusA)
	0.2% glycerol + 10 mM NH <sub>4</sub> Cl		$9.1 \pm 0.2$ (MsbA)
MY1905 $\Delta lacZ\Delta cat$	Glucose + cAA	$0.55 \pm 0.02$	$11.7 \pm 0.3$ (FusA)
	0.2% glucose + 0.2% casamino acids		$10.2 \pm 0.2$ (MsbA)

**Supplementary Table 4. The translation rates of FusA-LacZ and MsbA-LacZ under different growth rates.** The translation rate equals translation rate ( $\text{aa s}^{-1}$ ) / 336 (proteins mRNA $^{-1}$  s $^{-1}$ ) (Zarai et al., 2014), as the average length of proteins in *E. coli* is 336 amino acids (Gong et al., 2008). The elongation rate equals elongation rate ( $\text{aa s}^{-1}$ ) / 11 (sites s $^{-1}$ ) (Zarai et al., 2014), as each ribosome occupies about 11 residues in *E. coli* (10). All values are expressed as the mean  $\pm$  standard deviation of the mean of samples.

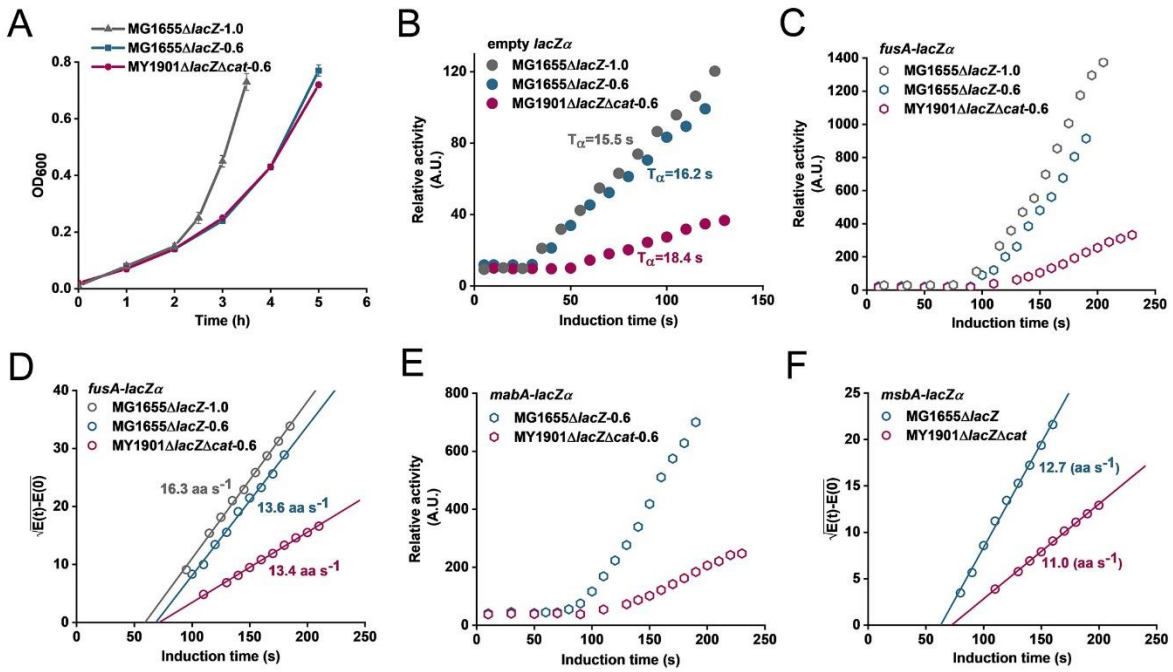
Strain	Growth rate ( $\text{h}^{-1}$ )	Translation rate (proteins mRNA $^{-1}$ s $^{-1}$ )	Elongation rate (sites s $^{-1}$ )	Initiation rate (sites s $^{-1}$ )
MG1655 $\Delta lacZ$	$1.10 \pm 0.04$	(FusA) $0.047 \pm 0.0003$	$1.47 \pm 0.01$	$0.049 \pm 0.0003$
		(MsbA) $0.045 \pm 0.0003$	$1.40 \pm 0.01$	$0.047 \pm 0.0003$
MG1655 $\Delta lacZ$	$0.55 \pm 0.03$	(FusA) $0.040 \pm 0.001$	$1.24 \pm 0.04$	$0.042 \pm 0.001$
		(MsbA) $0.038 \pm 0.001$	$1.15 \pm 0.03$	$0.039 \pm 0.001$
MY1901 $\Delta lacZ\Delta cat$	$0.55 \pm 0.02$	(FusA) $0.038 \pm 0.001$	$1.22 \pm 0.05$	$0.039 \pm 0.001$
		(MsbA) $0.032 \pm 0.001$	$1.00 \pm 0.03$	$0.033 \pm 0.001$



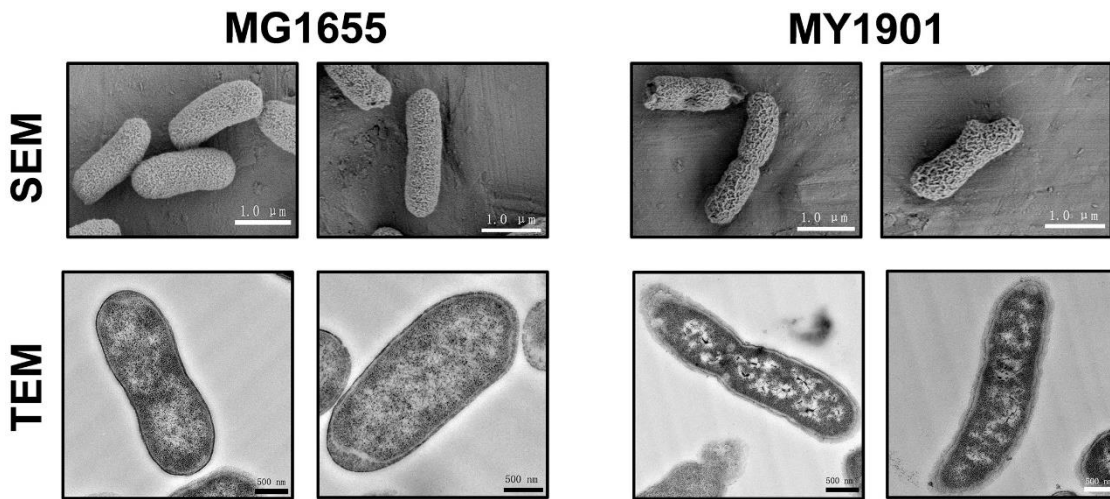
**Supplementary Figure 1** Growth curves of strains MY1901 and its evolved strain. Solid curves are the mean of three independent measurements and error bars represent the standard deviation of the mean of samples. All growth rates shown represent the mean  $\pm$  standard deviation of three independent experiments.



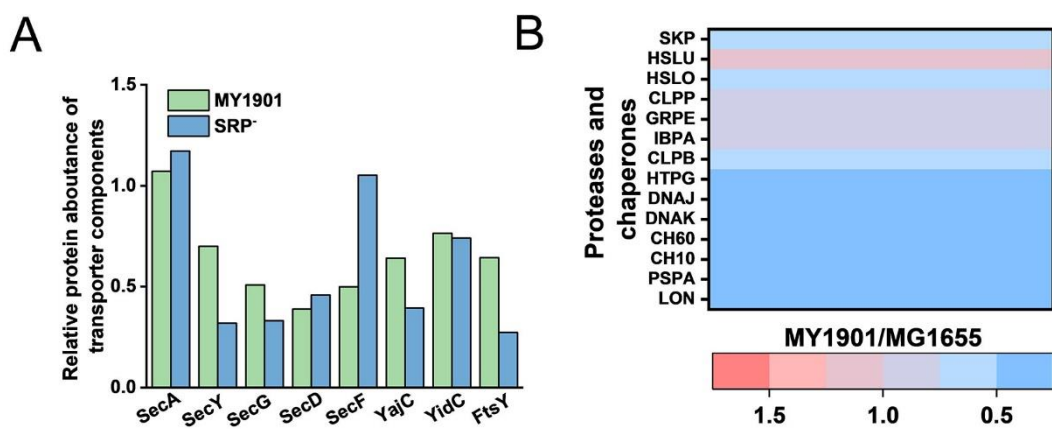
**Supplementary Figure 2** Predicted mRNA structures of the S10 leader. **(A)** RNA folding predicted hairpin structure of S10 leader with wild-type SD and the minimum free energy (MFE) of the thermodynamic ensemble ( $\Delta G$ ). **(B)** RNA folding predicted hairpin structure of S10 leader with mutant SD (SD\*) and the MFE and the  $\Delta G$ . The boxed region corresponds to the SD sequence.



**Supplementary Figure 3** Measurement of translational elongation rates of wild-type and suppressor cells. **(A)** Growth curves of strains in different MOPS medium. The growth rates of MG1655 $\Delta$ lacZ and MY1901 $\Delta$ lacZ $\Delta$ cat grown in the Glucose + cAA medium were approximately 1.0 h $^{-1}$  and 0.6 h $^{-1}$ , respectively. The growth rate of MG1655 $\Delta$ lacZ grown in Glycerol + NH<sub>4</sub>Cl medium was approximately 0.6 h $^{-1}$  (Supplementary Table S2). Solid curves are the mean of three independent biological replicates, and error bars represent the standard deviation value. **(B)** Calibration of the time cost of initiation steps by measuring the induction kinetics of the empty LacZ $\alpha$  fragment. **(C)** The induction curves of the LacZ $\alpha$  fused protein FusA-LacZ $\alpha$ . **(D)** The Schleif plot of the FusA-LacZ $\alpha$  protein was plotted against the induction time. **(E)** The induction curves of the LacZ $\alpha$  fused protein MabA-LacZ $\alpha$ . **(F)** The Schleif plot of the MabA-LacZ $\alpha$  protein was plotted against the induction time. Schleif plots were repeated three times with one typical result shown here.



**Supplementary Figure 4** Scanning electron microscopy (SEM) and transmission electron microscopy (TEM) analysis of the wild-type strain MG1655 and the suppressor strain MY1901. For SEM, the scale bar is 1.0  $\mu\text{m}$ . For TEM, the scale bar is 500 nM.



**Supplementary Figure 5** Fold changes in the expression of the components of transport machinery (A) and the heat shock response-related proteins (B) in strain MY1901 relative to that in strain MG1655 (Supplementary Data Set 1B and E).

## REFERENCES

- Blattner, F.R., Plunkett, G., 3rd, Bloch, C.A., Perna, N.T., Burland, V., Riley, M., Collado-Vides, J., Glasner, J.D., Rode, C.K., Mayhew, G.F., *et al.* (1997). The complete genome sequence of *Escherichia coli* K-12. *Science* 277, 1453-1462.
- Dai, X., Zhu, M., Warren, M., Balakrishnan, R., Okano, H., Williamson, J.R., Fredrick, K., and Hwa, T. (2018). Slowdown of Translational Elongation in *Escherichia coli* under Hyperosmotic Stress. *mBio* 9, e02375-02317.
- Gong, X., Fan, S., Bilderbeck, A., Li, M., Pang, H., and Tao, S. (2008). Comparative analysis of essential genes and nonessential genes in *Escherichia coli* K12. *Mol Genet Genomics* 279, 87-94.
- Lee, H.C., and Bernstein, H.D. (2001). The targeting pathway of *Escherichia coli* presecretory and integral membrane proteins is specified by the hydrophobicity of the targeting signal. *Proc Natl Acad Sci U S A* 98, 3471-3476.
- O'Connor, M., Goringe, H., and Dahlberg, A.E. (1992). A ribosomal ambiguity mutation in the 530 loop of *E. coli* 16S rRNA. *Nucleic Acids Research* 20, 4221-4227.
- Zarai, Y., Margaliot, M., and Tuller, T. (2014). Maximizing Protein Translation Rate in the Ribosome Flow Model: The Homogeneous Case. *IEEE/ACM Trans Comput Biol Bioinform* 11, 1184-1195.
- Zhang, D., and Shan, S.O. (2012). Translation elongation regulates substrate selection by the signal recognition particle. *J Biol Chem* 287, 7652-7660.
- Zhao, D., Yuan, S., Xiong, B., Sun, H., Ye, L., Li, J., Zhang, X., and Bi, C. (2016). Development of a fast and easy method for *Escherichia coli* genome editing with CRISPR/Cas9. *Microb Cell Fact* 15, 205.
- Zhao, L., Cui, Y., Fu, G., Xu, Z., Liao, X., and Zhang, D. (2021). Signal Recognition Particle Suppressor Screening Reveals the Regulation of Membrane Protein Targeting by the Translation Rate. *mBio* 12, e02373-02320.